

# Long-term response of respective grass types to variations in fire frequency in central Japan, inferred from phytolith and macrocharcoal records in cumulative soils deposited during the Holocene

Naoki Hayashi<sup>a\*</sup> • Tatsuichiro Kawano<sup>b</sup> • Jun Inoue<sup>a</sup>

<sup>a</sup>Department of Geosciences, Osaka City University, 3-3-138 Sugimoto, Sumiyoshi-ku, Osaka 558-8585, Japan

<sup>b</sup>West Japan Engineering Consultants, Inc., 1-1-1 Watanabe-dori, Chuo-ku, Fukuoka 810-0004, Japan

\*Corresponding author: Naoki Hayashi, E-mail: [yusayutyu@gmail.com](mailto:yusayutyu@gmail.com)

## Abstract

Phytolith and charcoal records in cumulative soils provide a past history of vegetation transition with fire occurrence. By using these records, we assess the long-term response of respective grass types to variations in fire frequency in central Japan. We analyzed phytoliths and macrocharcoals in cumulative soils on the Kannabe Plateau in central Japan. The results of the analysis showed that prior to 8000 cal BP, *Sasa* species was dominant along with *Pleioblastus* species under conditions of low fire frequency. Between 8000 and 2000 cal BP, the plateau was covered by grasslands dominated by *Pleioblastus* species under a warmer climate and/or an increase in fire frequency. Since approximately 2000 cal BP, the grasslands have been covered by *Miscanthus sinensis* under a high fire frequency of repeated cycles of annual burning, as is present today. The establishment and maintenance of a *M. sinensis* grassland are probably related to human activity in this area because this species had many uses. Correlation coefficients for phytolith types versus charcoal concentrations in cumulative soils from three areas in central Japan, including the Kannabe Plateau area, were obtained to assess the habitats and related fire frequencies for their respective grass types. These correlations were consistent with their fire tolerance and degree of succession, as inferred from modern observations. This suggests that the modern fire ecology of these grass types can be used to understand their long-term fire ecology.

## Keywords:

Fire frequency; Phytolith; Macroscopic charcoal; Grassland type; Cumulative soils: central Japan; Holocene

**The final, definitive version of this paper has been published in Quaternary International 2018 doi: 10.1016/j.quaint.2018.04.048 by Elsevier Ltd, All rights reserved. © 2018 Elsevier Ltd and INQUA.**

**This manuscript version is made available under the CC-BY-NC-ND 4.0 license**

<https://creativecommons.org/licenses/by-nc-nd/4.0/>

<https://www.sciencedirect.com/science/article/pii/S1040618218300302>

## **1. Introduction**

Fire plays an important role in the ecosystem, especially for flora (e.g., Bond et al., 2005) as it disturbs the vegetation. Because botanical tolerance or adaptability to fire is generally dependent on species, the vegetation type that develops in an area tends to correspond to the fire frequency in that area. Under natural conditions, fire frequency is usually determined by precipitation, temperature, vegetation type, and seasonal climatic variation, and fire occurs in an irregular manner. Fire is also artificially induced by human activity, which is generally repeated many times cyclically.

In Japan, very few wildfires occur naturally because of the high level of precipitation throughout the year. However, in some grassland areas, humans frequently induce fire for grassland maintenance. Maintained grasslands have likely been subjected to repeated fire cycles for hundreds of years or more (e.g., Iwaki, 1971), and the grassland types are presumably related to fire frequency. In these areas, fire frequency significantly influences the vegetation (especially herbaceous plants) over long timescales. However, a long-term relationship between fire frequency and specific vegetation types has yet to be fully established.

In Japan, phytolith and charcoal records in cumulative soils (andisols and paleosols) help in our understanding of the long-term vegetation transition (especially for grassland development and maintenance) and fire history of an area. Phytoliths are composed of biogenic silica that fill plant cell walls and survive the eventual decay of organic plant materials (Eguchi, 1998, Kawano et al., 2006). Macrocharcoal fragments (>100 µm) remain close to their source (fire area) before settling (e.g., Whitlock and Larsen, 2001). Thus, phytolith and charcoal records in cumulative soils provide a local history of vegetation type and fire. In this regard, many studies have clarified the vegetation transition and fire history in an area by use of such records (Takaoka and Yoshida, 2011, Okunaka et al., 2012, Kawano et al., 2012, Miyabuchi et al., 2012, Inoue et al., 2016). Inoue et al. (2016) summarized the results of a number of studies and indicated that phytolith assemblages are roughly related to

the charcoal influx in cumulative soils independent of location or age. Although they show that fire frequency largely determines the vegetation (grass) type in these areas, the response of respective grass species to variations in fire frequency has not been evaluated thoroughly.

To evaluate the response of respective grass types to changes in fire frequency, we examined phytolith assemblages and macrocharcoal particles in cumulative soils on the Kannabe Plateau, central Japan, where Japanese pampas grass (*Miscanthus sinensis*) grasslands have been maintained through repeated fire cycles for hundreds of years or more. The relationship between the percentages of respective phytolith morphotypes and associated charcoal concentrations were extracted from three grassland areas in central Japan (including the Kannabe Plateau). These areas are known to have been subjected to, which have been covered by grasslands through repeated fire cycles under similar climatic conditions, were then assessed statistically.

## 2. Study Site

The Kannabe Plateau is at an altitude of 350–450 m and is located north of Hyogo Prefecture in the Kinki region of central Japan (Fig. 1). The Kannabe Plateau contains a volcano, which last erupted approximately 20 ka ago (Tanase et al., 2002), and deposited scoria on top of the plateau. We sampled cumulative soils that formed on top of the scoria.

The mean annual temperature in the region is 12.3°C (1976–2015), with 2114 mm annual precipitation (1976–2015), measured at the Uwano Plateau Climatological Station (35°25'90" N, 134°35'00" E, elevation: 540 m), 10 km from the Kannabe Plateau. The eastern and southern parts of Kannabe Mountain are covered mainly by *M. sinensis* grassland, and the western and northern parts are covered by secondary forest of deciduous broad-leaved trees and Japanese red pines (*Pinus densiflora*) (Fig. 1). The warmth index (WI) is 97.1 and the cold index (CI) is -9.6 on the Kannabe Plateau. WI and CI were calculated as follows (Kira, 1991).  $WI = \sum (T_m - 5^\circ\text{C})$ , where  $T_m$  is the mean monthly temperature  $>5^\circ\text{C}$ , and  $CI = \sum (5^\circ\text{C} - T_m)$ , where  $T_m$  is the mean monthly temperature  $<5^\circ\text{C}$ . According to Kira (1991),  $WI > 85^\circ\text{C}$  is a warm temperate zone and  $WI < 85^\circ\text{C}$  is a cool temperate zone. Based on this climate classification, the Kannabe area is classified as a warm temperate zone close to the zone boundary.

Many ancient remains and archaeological sites have been found in an area adjacent to the Kannabe Plateau. The earliest remains of earthenware date back to the incipient Jomon period (Neolithic era prior to 10,000 cal BP). Some ancient burial grounds (tumulus) are located in the area, which were built in the 6th century. Manors have been developed since the 12th

century (Ota, 2001), and in the Edo era (the 17th to the 19th century) adjacent mountain areas of grasslands were likely developed here and maintained as meadows and pastures (Editorial committee of the history of Hidaka town, 1976).

### 3. Materials and Methods

#### 3.1. Materials

We collected soil samples from two sites (sites 1 and 2; Fig. 1) that were located in the *M. sinensis* grassland and at the boundary between the grassland and secondary forest, respectively.

In the soil profile at site 1 (35°30'10" N, 134°40'23" E), a black soil horizon was observed at a depth of 0–75 cm and a yellowish brown-grayish yellow soil occurred at a depth of 75–135 cm (Fig. 2). At site 2 (35°30'09" N, 134°40'27" E), a black soil horizon was at a depth of 0–130 cm and a yellowish brown horizon occurred at a depth of 130–148 cm (Fig. 2). The soil profiles were divided into 7 horizons at site 1 and 5 horizons at site 2, respectively. Characteristics of the respective horizons are shown in Supplementary table 1. We collected approximately 10 cm thick samples from the soil profile at each site, so that each sample consisted of a single soil horizon, except for the surface soil layer at site 2 (0–20 cm depth). The surface layer there was very loose and included numerous twigs and roots, indicating that the soil was mainly composed of recently redeposited materials. Thus, we did not use surface soil in this study.

#### 3.2. Radiocarbon dating

We used three macrocharcoal samples and two bulk soil (total organic carbon) samples for radiocarbon dating (Table 1). AMS radiocarbon dating was performed by Beta Analytic Inc. (Miami, FL, USA). Extraction and pretreatment procedures of the samples used for AMS dating are described below.

Macrocharcoals were extracted from soils as follows. We collected 50 g subsamples from each soil sample. First, 1.2N NaOH was added to each subsample and heated at 130°C for 3 h. Then the samples were gently washed through a sieve (mesh size: 125 µm) and each residue (>125 µm) was collected. We repeated this process until the supernatant liquid is clear. After that, 1.2N HCl was added and heated at 130°C for 3 h. Then the samples were gently washed through a sieve (mesh size: 125 µm) and each residue was collected. We repeated this process until the supernatant liquid is clear. The supernatant liquid including plant fragments was removed using an aspirator and we collected macrocharcoals. The

collected macrocharcoal samples were pretreated as follows. The samples were saturated in de-ionized water at 70°C. Then the samples were repeated soakings of 0.1N HCl for 1-2 h to eliminate any carbonates. After rinsing to neutral in de-ionized water, a solution of 1-2% NaOH was then applied at 70°C for 2-4 h and this process was repeated until the supernatant liquid is clear. The samples were again rinsed to neutral with de-ionized water, and a final acid wash (0.5-1.0N HCl) was applied at 70°C for one hour to ensure the alkali was neutralized. The samples were then and once again rinsed to neutral with de-ionized water. The sample pretreatment was applied by Beta Analytic Inc..

Soil samples were pretreated as follows. Soil samples were dispersed in de-ionized water and homogenized through stirring and sonication, and then sieved through 180 µm sieves. The materials passing through the sieve were used for the analysis. The materials were bathed in 1.25N HCl at 90°C for a minimum of 1.5 h to ensure removal of carbonates. These were followed by serial de-ionized water rinses at 70°C until neutrality was reached. Any debris or micro-rootlets were discarded during these rinses. The sample pretreatment was applied by Beta Analytic Inc..

Radiocarbon dates (BP) were obtained after the correction using  $\delta^{13}\text{C}$  (Table 1). We calibrated the dates to calendar years (cal BP) using the Calib Rev 7.0.4 program (<http://calib.qub.ac.uk/calib/calib.html>) and the IntCal13 calibration dataset (Reimer et al., 2013).

Based on the dates obtained from site 1, sedimentation rates were calculated by assuming constant sedimentation rates between the dated points in the soils and that at the age of 0 cm depth (top of the soils; 0 cal BP); the sedimentation rate of the soils below 72 cm depth was  $0.03 \text{ cm}\cdot\text{y}^{-1}$ , that of the soils between 25 to 72 cm depth was  $0.008 \text{ cm}\cdot\text{y}^{-1}$ , and that of the soils above 25 cm depth was  $0.01 \text{ cm}\cdot\text{y}^{-1}$ .

### 3.3. *Phytolith analysis*

We collected 1 cm<sup>3</sup> subsamples from each soil sample to extract phytoliths following the method of Kawano et al. (2007). Prior to a chemical treatment, we added about 200,000 glass beads (45 µm diameter) to each subsample to estimate the phytolith concentration (Fujiwara, 1976). We extracted phytoliths from the soil by the oxidation of organic matter using 30% H<sub>2</sub>O<sub>2</sub>. Calcium carbonate was removed using 3N HCl, and clay was removed according to Stokes' law. We mounted phytoliths on a glass slide with Eukitt and observations were made with a microscope at  $\times 400$  magnification. We identified and counted phytoliths until we had counted at least 400 phytoliths (800-1700 phytoliths, except three samples). We identified

phytoliths according to The International Code for Phytolith Nomenclature 1.0 (Madella et al., 2005), and classified bulliform cells and some short cells into subcategory-types, based on the methods reported by Miyabuchi and Sugiyama (2006), Kawano (2008), Kondo (2010), Okunaka et al. (2012), and Kawano et al. (2012) (Fig. 3). Then the percentages of respective phytolith types were calculated. Their standard errors (SE) are generally estimated to be approximately one percentage at the most, although the SE depends on the total number of counted phytoliths in a sample and the percentage of each phytolith type. Because the 95% confidence interval is constructed by the percentage  $\pm 1.96 \times \text{SE}$ , the confidence intervals for the percentages of respective phytolith types are assumed to be the respective percentages  $\pm$  equal to or less than a few percentages.

### 3.4 Macrocharcoal analysis

We extracted macrocharcoal fragments from the soil samples by following the method of Okunaka et al. (2012). We collected 0.5 cm<sup>3</sup> subsamples from each soil sample. Ten percent KOH was first added to each sample and 24 h later the samples were gently washed through a sieve (mesh size: 125  $\mu\text{m}$ ). To each residue ( $>125 \mu\text{m}$ ), 7.5% HCl was added and the samples were left for 24 h to disperse the particles. The samples were then gently washed through a series of nested sieves (mesh sizes: 125  $\mu\text{m}$ , 250  $\mu\text{m}$ , and 1 mm) to yield 125–250  $\mu\text{m}$ , 250  $\mu\text{m}$ –1 mm, and  $>1 \text{ mm}$  fractions. All of the charcoal particles in each subsample, which were recognized as black, opaque, or angular particles showing cellular features, were identified and counted under a stereomicroscope at  $\times 40$  magnification. Charcoal abundance (particles $\cdot\text{cm}^{-3}$ ) was calculated from these data.

## 4. Results

### 4.1 Phytolith analysis

Fig. 4 shows the percentage of each phytolith-type occurrence and phytolith concentration at sites 1 and 2. A cluster analysis was applied to the phytolith assemblages (percentage of respective phytolith types, except unidentified phytoliths) at both sites to identify phytolith assemblage zones and their similarity between the sites (Fig. 5). Based on the results of this analysis, four phytolith zones were established at each site (1-1, 1-2, 1-3, and 1-4 at site 1, and 2-1, 2-2, 2-3, and 2-4 at site 2). The phytolith assemblages in zones 1-1, 1-2, 1-3, and 1-4 were similar to the respective zones 2-1, 2-2, 2-3, and 2-4, as shown by the cluster analysis.

In 1-1 and 2-1 (135–85 cm depth at site 1 and 148–130 cm depth at site 2), *Sasa*-type bulliform cell phytoliths were dominant (26%–35%). Percentages of *Pleioblastus*-type

bulliform cell phytoliths were generally low (7%–14%) and few Andropogoneae-type bulliform cell phytoliths occurred (<3%). Bambusoid-type short cell phytoliths accounted for a large proportion of the short cell phytoliths (19%–24%). Elongate- and Acicular-type phytoliths were also common; however, the concentrations were lower than in other zones (Elongate: 4%–10%, Acicular: 2%–6%). Jigsaw puzzle-shaped phytoliths were absent, except for one sample (<1%).

Zones of 1-2 and 2-2 (85–63 cm depth at site 1, 130–120 cm depth at site 2) were characterized by roughly equal percentages of *Sasa*-type bulliform cell phytoliths (13%–21%) and *Pleioblastus*-type bulliform cell phytoliths (14%–21%). In these zones, the percentage of *Sasa*-type bulliform cell phytoliths decreased gradually with depth, whereas those of *Pleioblastus*-type bulliform cell phytoliths increased gradually. Few Andropogoneae-type bulliform cell phytoliths occurred (1%–5%). Bambusoid short cell phytoliths were dominant (16%–27%) and other short cell phytoliths were scarce (<1%). The percentages of Elongate-type phytoliths were high relative to 1-1 and 2-1 (14%–17%). Jigsaw puzzle-shaped phytoliths were rare, or absent altogether in this zone (<1%).

In 1-3 and 2-3 (63–35 cm depth at site 1 and 120–50 cm depth at site 2), *Pleioblastus*-type bulliform cell phytoliths were dominant (16%–21%) instead of *Sasa*-type bulliform cell phytoliths (4%–12%). In addition, Bambusoid short cell phytoliths and Elongate-type phytoliths were abundant (Bambusoid: 15%–23%, Elongate: 17%–26%). Jigsaw puzzle-shaped phytoliths were scarce in this zone (<1%).

The 1-4 and 2-4 (35–0 cm depth at site 1 and 50–20 cm depth at site 2) sites were characterized by the highest percentages of Andropogoneae bulliform cell phytoliths and Bilobate short cell phytoliths (Andropogoneae-type: 5%–14%, Bilobate: 2%–4%). Percentages of *Pleioblastus*-type bulliform cell phytoliths were also high (12%–16%). Bambusoid short cell phytoliths and Elongate-type phytoliths were abundant, similar to 1-3 and 2-3 zones (Bambusoid: 23%–31%, Elongate: 20%–25%). Jigsaw puzzle-shaped phytoliths were scarce in this zone (<1%).

#### 4.2 Macrocharcoal analysis

Macrocharcoal concentrations at sites 1 and 2 are shown in Fig. 4. Here, we treated the number of charcoal particles from 125  $\mu\text{m}$  to 1 mm in size (sum of the 125–250  $\mu\text{m}$  and 250  $\mu\text{m}$  to 1 mm sized particles) included in a 1  $\text{cm}^3$  soil sample as the macrocharcoal concentration. In the lower soil layers at each site (135–75 cm depth at site 1 and 148–120 cm depth at site 2), macrocharcoal concentrations were low (20–430 particles $\cdot\text{cm}^{-3}$  at site 1 and

340–1000 particles·cm<sup>-3</sup> at site 2). In the middle soil layers, the macrocharcoal concentration increased upward at each site (820–1370 particles·cm<sup>-3</sup> at 75–35 cm depth at site 1 and 2070–3370 particles·cm<sup>-3</sup> at 120–40 cm depth at site 2). In the upper soil layers (35–0 cm depth at site 1 and 40–20 cm depth at site 2), macrocharcoal concentrations were generally high (1710–1760 particles·cm<sup>-3</sup> at site 1 and 2990 particles·cm<sup>-3</sup> at site 2).

## 5. Discussion

### 5.1 Vegetation transition and fire history on the Kannabe Plateau

Based on the characteristics of the phytolith assemblages, four zones were recognized at each site (1-1, 1-2, 1-3, and, 1-4 at site 1, and 2-1, 2-2, 2-3, and 2-4 at site 2), and respective zones at each site were well correlated with each other, as mentioned above (Fig. 4). The radiocarbon dates obtained at each site were broadly consistent with the correlation of the zones; ages obtained in the lower part of 1-1 and 2-1 were ~9000–10000 cal BP and those in 1-4 and 2-4 were ~1000–2000 cal BP. These facts indicate that the vegetation transitions both at sites 1 and 2 occurred similarly and contemporaneously. It implies that the phytolith assemblages obtained in this study probably represent vegetation types in the sampling sites and their adjacent areas (probably at least the southern part of the Kannabe Plateau). Based on the radiocarbon dates and sedimentation rates at site 1, the ages of the respective zones were roughly estimated as follows: 1-1 and 2-1 are prior to 9000 cal BP; 1-2 and 2-2 are 9000–6000 cal BP; 1-3 and 2-3 are 6000–3000 cal BP; 1-4 and 2-4 are after 2000 cal BP. Considering the ages of these zones, changes in vegetation and habitat in this area were evaluated from the phytolith assemblages and charcoal concentrations in the respective zones.

Bulliform cell phytoliths of *Sasa*-type, *Pleioblastus*-type, and Andropogoneae-type were produced from only the genus and subfamily, respectively (Kondo and Sase, 1986, Sugiyama and Fujiwara, 1986), whereas the short cell phytoliths do not correspond completely to the grass subfamily. Thus, we reconstructed the vegetation transition mainly focusing on the changes in bulliform cell phytoliths. A certain percentage of either/both *Sasa*-type, *Pleioblastus*-type, or/and Andropogoneae-type in all samples suggests that these vegetation types flourished at the sampling sites. In addition, Jigsaw puzzle-shape phytoliths, which are produced from broad-leaf trees, were scarce in all zones. These facts indicate that grasslands of either/both *Sasa*-type, *Pleioblastus*-type, or/and Andropogoneae-type developed on the plateau during the Holocene.

The charcoal concentration generally increased upward at both sites, and in 1-4 and 2-4



macrocharcoal fragments were abundant. In modern times, *M. sinensis* grasslands in this area have been maintained by annual grassland burning. Thus, the abundant macrocharcoal in the uppermost soils reflect a modern annual burnings. Given this fact, the charcoal concentration is considered to roughly represent fire frequency.

In the soils deposited prior to approximately 9,000 cal BP (Kannabe Plateau 1-1 and 2-1), *Sasa*-type bulliform cell phytoliths and Bambusoid short cell phytolith were dominant with *Pleioblastus*-type bulliform cell phytoliths, and the macrocharcoal concentration was low, indicating that *Sasa* species flourished with *Pleioblastus* species under the conditions of low fire frequency during this period. In Japan, without any disturbance, grasslands tend to shift to forest because of the favorable climate conditions for arboreal growth. However, our results show that *sasa* species presumably stood on the plateau prior to approximately 9,000 cal BP without any disturbance. This is possibly because of the poor soil that developed on the scoria deposits, retarding forest development.

The 1-2 and 2-2 zones of 9000–6000 cal BP were characterized as having almost equal percentages of *Sasa*-type bulliform cell phytoliths and *Pleioblastus*-type bulliform cell phytoliths with low or intermediate charcoal concentrations. This indicates that both *Sasa* and *Pleioblastus* species flourished under moderate or low fire frequency conditions. These zones were placed as transition periods from *Sasa* dominance (1-1 and 2-1) to *Pleioblastus* dominance (1-3 and 2-3). Under a warm temperate climate, *Pleioblastus* species tend to flourish more than *Sasa* species (Shimada et al., 1973). In addition, *Pleioblastus* species are generally more tolerant of disturbance (such as fire) than *Sasa* species (Shimada et al., 1973). Considering these habitats, the expansion of *Pleioblastus* species and contraction of *Sasa* species were probably due to climatic warming in this period with relatively few fire disturbances. Climatic warming was shown by palynological data in the coastal area 20 km distance from the study sites; during this period, an evergreen forest of ring-cupped oaks (*Cyclobalanopsis* species) developed and was replaced with a deciduous oak forest (Maeda et al., 1989).

In 1-3 and 2-3 of 6000–3000 cal BP, *Pleioblastus*-type bulliform cells were dominant with intermediate to high charcoal concentrations, indicating that *Pleioblastus* species were predominant under a moderate to high fire frequency. *Pleioblastus* species are somewhat tolerant to disturbance, and from modern observations, they tend to flourish under a conditions of moderate disturbance frequency of disturbance, e.g., weeding, grazing and fires (Shimada et al., 1973). For instance, modern observation of chino bamboo (*Pleioblastus chino* var. *viridis*, a representative *Pleioblastus* variety distributed in western Japan), they

would have flourished under the conditions of disturbance (weeding) conditions with a 2–3 year or less frequency (Shigematsu, 1985). This is consistent with our suggestion that *Pleioblastus* species flourished under a moderate to high fire frequency.

Zones 1-4 and 2-4 after 2000 cal BP were characterized by high percentages of Andropogoneae-type bulliform cell phytoliths and Bilobate short cell phytoliths, which were produced by Andropogoneae species, accompanied with an abundant macrocharcoal. By contrast, very few *Sasa*-type bulliform cell phytoliths were found in these zones. These findings indicate that Andropogoneae species flourished more during this period than during other periods and were probably predominant. In modern times, *M. sinensis* grasslands have remained on the plateau with annual cycles of intentional burning. Both Andropogoneae-type bulliform cell phytoliths and Bilobate short cell phytoliths are produced from *M. sinensis*, and it is assumed that the frequent burning produced abundant charcoal particles. Here, we infer imply that *M. sinensis* grasslands persisted on the plateau during past after 2000 cal BP. This inference is consistent with the fact that Andropogoneae grasslands generally develop under conditions of repeated fire cycles (e.g., Iwaki, 1971).

Inoue et al. (2016) suggested a relationship between macrocharcoal flux and primary phytolith assemblage in cumulative soils in respective areas in Japan. We calculated the macrocharcoal fluxes at site 1, where three radiometric ages were obtained, to assess the relationship between macrocharcoal flux and primary phytolith assemblage at the study site. The number of charcoal fluxes ( $\text{particles}\cdot\text{cm}^{-2}\text{y}^{-1}$ ) was estimated by multiplying the charcoal concentration ( $\text{particles}\cdot\text{cm}^{-3}$ ) by the sedimentation rate ( $\text{cm}\cdot\text{y}^{-1}$ ). Macrocharcoal fluxes in the phytolith zone 1-1 were  $<10\text{ particles}\cdot\text{cm}^{-2}\text{y}^{-1}$ , except for one data point at the 93–103 cm depth ( $10.4\text{ particles}\cdot\text{cm}^{-2}\text{y}^{-1}$ ); those in the 1-2 and 1-3 phytolith zones were 7–10  $\text{particles}\cdot\text{cm}^{-2}\text{y}^{-1}$ , except for two data points at the 75–85 cm depth ( $13.0\text{ particles}\cdot\text{cm}^{-2}\text{y}^{-1}$ ) and the 69–75 cm depth ( $15.5\text{ particles}\cdot\text{cm}^{-2}\text{y}^{-1}$ ). These exceptional fluxes are probably nominal values due to the high sedimentation rate in the lower parts of the soils. Macrocharcoal fluxes in phytolith zone 1-4 were very high ( $19\text{--}20\text{ particles}\cdot\text{cm}^{-2}\text{y}^{-1}$ ). These findings suggest that at the study site, *Sasa* species and *Pleioblastus* species had flourished under a low to moderate fire frequency, as represented by low charcoal fluxes of  $<10\text{ particles}\cdot\text{cm}^{-2}\text{y}^{-1}$ , and *M. sinensis* grasslands were maintained with a high fire frequency, and represented by high charcoal fluxes of  $>10\text{ particles}\cdot\text{cm}^{-2}\text{y}^{-1}$ . The relationship between the primary phytolith assemblage (or vegetation type in the ages) and macrocharcoal flux found in this study agrees with the suggestion of Inoue et al. (2016).

### 5.2 Comparison between vegetation transition and historical records

Our phytolith and charcoal records in cumulative soils cover approximately 10,000 years, which corresponds to the historical era since the early Jomon Era. In the area adjacent to the study sites, many human remains from the Jomon Era have been found. The Jomon culture was characterized by a hunting and gathering lifestyle from 15000 to 2300 cal BP. Thus, the increase in fire frequency implied in our study is broadly consistent with the known culture context for the region.

In the adjacent area, rice cropping started in 2000 cal BP, during Yayoi Era, and since the Kamakura Era (the 12th century; Ota, 2001), manors were developed. At that time the population would have increased, and crop fields would have been developed. In ancient Japan, *M. sinensis* was used as a building material (e.g., thatch for roofing) and as a fertilizer (e.g., Iwaki, 1971; Tsujino, 2011). It is assumed that demand for the grass increased in this area as the manors developed. Our findings indicate that the development of *M. sinensis* grasslands is consistent with frequent burning on the Kannabe Plateau since the ancient or middle ages, including the period of manor development.

### 5.3 Vegetation type responses to variations in fire frequency over the long-term in central Japan

To evaluate how respective vegetation types responded to changes in fire frequency over the long-term in central Japan, the percentages of dominant respective phytolith morphotypes and charcoal concentrations obtained from three areas in central Japan (Kannabe Plateau in this study, Soni Plateau reported by Okunaka et al., 2012, and the Tonomine Plateau reported by Inoue et al., 2016; Fig. 1) were assessed by Spearman's rank correlations coefficients. *M. sinensis* grasslands are typical in modern times, and these have likely been maintained through repeated cycles of fire for at least ~1000 years, as suggested by records of phytolith assemblages and charcoal in cumulative soils. The elevations and climatic conditions of these areas are similar to each other; elevations, annual mean temperature, and annual precipitation on the Kannabe Plateau are ~400 m, 12.3°C, and 2114 mm, respectively, those on the Soni Plateau are ~700 m, 12.7°C, and 1728 mm, respectively, and those on the Tonomine Plateau are ~800 m, 13.1°C, and 2021 mm, respectively. These areas are located close to the boundary between a warm temperate zone and a cool temperate zone, enabling *Sasa* species, *Pleioblastus* species, and *M. sinensis* to stand, each of which has a specific degree of succession (DS) and a particular fire-adaptability. The similar climatic and other conditions provide an ideal situation to assess the response of respective vegetation types to variations in

fire frequency by use of the phytolith and charcoal records.

We calculated Spearman's rank correlations coefficients between the percentage of each morphotype and macrocharcoal concentration in each sample at respective sites (at two sites in each of the three areas) (Table 2). For the calculation, the phytolith morphotypes were limited to that observed over 30 grains in at least one sample at all of the sites. The correlation coefficients for each morphotype in the respective areas were largely similar, with some exceptions, e.g., the Bilobate-type on the Soni Plateau and the *Pleioblastus*-type and Bambusoid-type on the Tonomine Plateau. This indicates that the correlations between percentages of phytolith type and charcoal concentrations could be recognized as typical ones in the respective areas. The correlations coefficients for the Andropogoneae-type and Bilobate-type were generally high at all of the sites (0.7–1.0 and 0.3–0.8, respectively). By contrast, the coefficient for the *Sasa*-type was generally low (-1.0–0.1), except for the Soni Plateau site 2. The coefficient for the *Pleioblastus*-type was moderate (-0.6–0.6) with high *p* values. The coefficients for Bambusoid-type and Elongate-type were variable (-0.9–0.5 and -0.8–0.9, respectively).

As mentioned above, both the Andropogoneae-type and Bilobate-type were produced by Andropogoneae species including *M. sinensis*, which presumably flourished for ~1000 years in these areas. Thus, most of the Andropogoneae- and Bilobate-types could have come from *M. sinensis*. Modern observations suggest that *M. sinensis* grasslands are prone to develop and be sustained under frequent fire conditions, e.g., annual burnings (e.g., Iwaki, 1971; Shimada et al., 1973; Yamane, 1973). A *M. sinensis* community has a low DS relative to a *Sasa* community and *Pleioblastus* community (Numata, 1969). The high coefficients for Andropogoneae- and Bilobate-types produced by *M. sinensis* suggest that the natural tendency of *M. sinensis* to flourish under fire-prone conditions is recognized even in the hundreds or thousands of years timescale. That is *M. sinensis* largely flourishes more as fire frequency increases, even over the long-term. Because fire disturbance resets vegetation succession, frequent fires have repeatedly prevented this succession, resulting in the maintenance of *M. sinensis* grasslands.

The percentages of the *Sasa*-type, which is produced only by *Sasa* species (Kondo and Sase, 1986; Sugiyama and Fujiwara, 1986), were negatively correlated with charcoal concentrations, as indicated by low coefficients for the type. *Sasa* species are generally more sensitive to fire than *M. sinensis* and *Pleioblastus* species; *Sasa* species are prone to establish under conditions of less disturbance such as fire (Shimada et al., 1973). The DS of the *Sasa* community is generally lower than the *M. sinensis* community and *Pleioblastus* community

(Numata, 1969). Based on these facts, the negative correlations between the percentage of *Sasa* species and charcoal concentration suggest that in the long term, *Sasa* species tend to flourish stably under fire-free or low fire frequency conditions.

The moderate coefficients with high  $p$  values for the *Pleioblastus*-type revealed little or no correlation between percentages of the type and charcoal concentrations. *Pleioblastus* species are generally somewhat tolerant to disturbances (e.g., Shimada et al., 1973). The DS of the *Pleioblastus* community is higher than that of the *M. sinensis* community but lower than that of the *Sasa* community (Numata, 1969). This suggests that *Pleioblastus* species generally flourish under a condition of moderate disturbance frequency (probably every several years or possibly more). Little or no correlation between the percentages of the type and charcoal concentrations indicate that a moderate DS for the species could result in either an expansion or contraction of the species with fire frequency, as fire frequency changes over the long-term. We believe that a moderate fire frequency of several years or more resets the vegetation succession, resulting in the longer duration of *Pleioblastus* species flourishing in a period. By contrast, under a high fire frequency, the fire prevents the transition to a *Pleioblastus* community is interrupted by repeated fire; while under a low fire frequency, the *Pleioblastus* communities tend to shift to other vegetation types, with a high DS, e.g., a *Sasa* community.

Correlation coefficients for Bambusoid- and Elongate-types were variable, which are types produced by multiple taxa (genus and family, respectively) (Sase and Kondo, 1974; Kondo and Otaki, 1992; Twiss et al., 1969). The source of the Bambusoid-type is *Sasa* species and *Pleioblastus* species, which have remained during most periods in the last 10,000 years in these areas. The Elongate-type is produced by various species, the source of which cannot be identified.

As mentioned above, Spearman's rank correlations coefficients between the percentage of each morphotype and macrocharcoal concentration were well consistent with the DS of each species and its fire tolerance established from modern observations. This suggests that fire tolerance and the DS of respective vegetation types observed in modern times would contribute significantly to the long-term contraction and expansion of the respective vegetation types under changing fire frequencies.

## **6. Conclusion**

We analyzed phytoliths and macrocharcoal in cumulative soils of the Kannabe area to assess the long-term response of grass types to variations in fire frequency in central Japan. The results of the analyses showed that the vegetation transition and fire history on the Kannabe

Plateau during the Holocene prior to 8,000 years ago was dominated by *Sasa* species under a low fire frequency. Between 8,000 and 2,000 years ago, the grassland was dominated by *Pleioblastus* species, and the *M. sinensis* grassland has been sustained by annual intentional fires since ~2,000 years.

The correlation coefficients for respective phytolith types versus charcoal concentrations in cumulative soils in three areas including the Kannabe Plateau area were obtained to assess the habitats related to fire of their respective grasses. The correlation coefficients for Andropogoneae-type and Bilobate phytolith percentages were strongly positive, by contrast, the correlation coefficient for *Sasa*-type phytoliths was negative. The correlation coefficients for *Pleioblastus*-type percentages varied depending on the area. These results agree with their fire tolerances differences and the DS inferred from modern observations.

### **Acknowledgement**

We thank Prof. Mitamura M. for helpful suggestions. We thank the anonymous reviewers for their careful reading of our manuscript and their many insightful comments and suggestions. This study was partially supported by Grant-in-aid for science research in San'in Kaigan UGGp (to N. Hayashi) and Grants-in-Aid for Scientific Research from the Ministry of Education, Culture, Sports, Science and Technology of Japan (No. 16K07646 to J. Inoue).

### **References**

- Bond, W. J., Woodward, F. I., Midgley, G.F., 2005. The global distribution of ecosystems in a world without fire. *New Phytologist* 165, 525-538.
- Editorial committee of the history of Hidaka town., 1976. The first volume of the history of Hidaka town. Hidaka town (in Japanese).
- Eguchi, S., 1998. Distribution of opal phytoliths and their mother plants in the coastal zone of Japan. *Japanese Journal of Ecology* 48, 245-255 (in Japanese, with English abstract).
- Fujiwara, H., 1976. Fundamental studies of plant opal analysis: on the silica bodies of motor cell of rice plants and their near relatives, and the method of quantitative analysis. *Archaeology and Natural Science (Biannual Journal of the Japanese Societies on Cultural Property)* 9, 15-29 (in Japanese).
- Inoue, J., Okunaka, R., Kawano, T., 2016. The relationship between past vegetation type and fire frequency in western Japan inferred from phytolith and charcoal records in cumulative soils. *Quaternary International* 397, 513-522.
- Iwaki, H., 1971. Ecology of grassland. Kyoritsu Shuppan, Tokyo (in Japanese).

- Kawano, T., 2008. Morphology of leaf phytoliths in selected tree species of Japan. *Bulletin of the Kyoto Prefectural University Forests* 49, 19-31 (in Japanese).
- Kawano, T., Kawano, K., Udatsu, T., Fujiwara, H., 2006. Relationships between modern tree phytolith assemblages and tree composition in lucidophyllous forests in the southern part of Miyazaki Prefecture. *Japanese Journal of Historical Botany* 14, 3-14 (in Japanese, with English abstract).
- Kawano, T., Sasaki, N., Hayashi, T., Takahara, H., 2012. Grassland and fire history since the late-glacial in northern part of Aso Caldera, central Kyusyu, Japan, inferred from phytolith and charcoal records. *Quaternary International* 254, 18-27.
- Kawano, T., Takahara, H., Nomura, T., Shibata, H., Uemura, S., Sasaki, N., Yoshioka, T., 2007. Holocene phytolith record at *Picea glehnii* stands on the Dorokawa Mire in northern Hokkaido, Japan. *The Quaternary Research* 46, 413-426.
- Kira, T., 1991. Forest ecosystems of east Asia and southeast Asia in a global perspective. *Ecological Research* 6, 185-200.
- Kondo, R., 2010. Phytolith atlas. Hokkaido University Press, Sapporo (in Japanese).
- Kondo, R., Otaki, M., 1992. The short cell phytoliths in lamina of bambusoideae. The report of Fuji bamboo botanical garden 36, 23-43 (in Japanese).
- Kondo, R., Sase, T., 1986. Opal Phytolith, their Nature and Application. *The Quaternary Research* 25, 31-63 (in Japanese).
- Madella, M., Alexandre, A., Ball, T., 2005. International code for phytolith nomenclature 1.0. *Annals of Botany* 96, 253-260.
- Maeda, Y., Nakai, N., Matsumoto, E., Nakamura, T., Kusunoki, S., Matsushima, Y., Satou, Y., Matsubara, A., Kumano, S., Kuromi, M., Nukata, M., Aoki, T., Furuta, N., Kobashi, T., Matsui, J., Kawahara, N., Yamashita, H., 1989. Holocene, environmental changes in the Kei lowland, Hyogo prefecture, eastern part of San-in coast district, Japan. *Ritsumeikan chirigaku* 1, 1-19 (in Japanese).
- Miyabuchi, Y., Sugiyama, S., 2006. A 30,000-year Phytolith Record of a Tephra Sequence, East of Aso Caldera, Southwestern Japan. *The Quaternary Research* 45, 15-28 (in Japanese, with English abstract).
- Miyabuchi, Y., Sugiyama, S., Nagaoka, Y., 2012. Vegetation and fire history during the last 30,000 years based on phytolith and macroscopic charcoal records in the eastern and western areas of Aso Volcano, Japan. *Quaternary International* 254, 28-35.
- Numata, M., 1969. Progressive and retrogressive gradient of grassland vegetation measured by degree of succession-Ecological judgement of grassland condition and trend IV. *Vegetation*

19, 96-127.

- Okunaka, R., Kawano, T., Inoue, J., 2012. Holocene history of intentional fires and grassland development on the Soni Plateau, Central Japan, reconstructed from phytolith and macroscopic charcoal records within cumulative soils, combined with paleoenvironmental data from mire sediments. *The Holocene* 22, 793-800.
- Ota, J., 2001. The minor of Tajima. In Amino, Y., Ishii, S., Inagaki, Y., Nagahara, K. (Eds), *Japanese minor history 8 the minor of Kinki region 3*. Yoshikawakobunkan, Tokyo, pp. 243-289 (in Japanese).
- Reimer, P.J., Bard, E., Bayliss, A., Beck, J.W., Blackwell, P.G., Ramsey, C.B., Brown, D.M., Buck, C.E., Edwards, R.L., Friedrich, M., Grootes, P.M., Guilderson, T.P., Haflidason, H., Hajdas, I., Hatte, C., Heaton, T.J., Hogg, A.G., Hughen, K.A., Kaiser, K.F., Kromer, B., Manning, S.W., Reimer, R.W., Richards, D.A., Scott, E.M., Southon, J.R., Turney, C.S.M., van der Plicht, J., 2013. Selection and treatment of data for radiocarbon calibration: an update to the international calibration (Intcal) criteria. *Radiocarbon* 55, 1923-1945.
- Sase, T., Kondo, R., 1974. The study of opal phytoliths in the humus horizon of buried volcanic ash soils in Hokkaido. *Research bulletin of Obihiro University* 8, 465-483 (in Japanese, with English abstract).
- Shigematsu, T., 1985. An ecological study on Management of *Pleioblastus chino var. viridis* type floor in recreation forest. *Journal of the Japanese Institute of Landscape Architects* 48, 145-150 (in Japanese, with English abstract).
- Shimada, Y., Kawabe, S., Kayama, R., Itoh, S., 1973. *Ecology of grassland*. Tsukiji Shokan, Tokyo (in Japanese).
- Sugiyama, S., Fujiwara, H., 1986. The shape of silica bodies in the motor cells of Bambusoideae. *Archaeology and Natural Science* 19, 69-84 (in Japanese).
- Tanase, A., Ishimaru, T., Furusawa, A., Ninomiya, A., Martin, A. J., 2002. Tephrochronology of the Tada and Kannabe Volcanoes, Kannabe Monogenetic Volcano Group, Hyogo Prefecture, Southwest Japan. *The geological society of Japan conference 109*. The geological society of Japan, Tokyo, pp. 228 (in Japanese).
- Takaoka, S., Yoshida, S., 2011. *Miscanthus*-grassland history in the Sengokubara area of Hakone-machi, central Japan, inferred from phytolith and charcoal records. *The Quaternary Research* 50, 319-325 (in Japanese, with English abstract).
- Tsujino, R., 2011. The history of relations between human and nature in Japan. In Yumoto, T. (Eds) *What is environmental history?* Bunichisougousyuppan, Tokyo (in Japanese), pp. 33-51.



- Twiss, P. C., Suess, E. Smith, R. M. 1969. Morphological classification of grass phytoliths. *Soil Science Society of America* 33, 109-115.
- Whitlock, C., Larsen, C., 2001. Charcoal as a fire proxy. In: Smol, J.P., Birks, H.J.B., Last, W.M. (Eds.), *Terrestrial, Algal, and Siliceous Indicators, Tracking Environmental Change Using Lake Sediments*, vol. 3. Kluwer Academic Publisher, Dordrecht, pp. 75-97.
- Yamane, I., 1973. The meaning of *Miscanthus sinensis* in the formation of kuroboku soil. *Pedologist* 17, 16-26 (in Japanese, with English abstract).

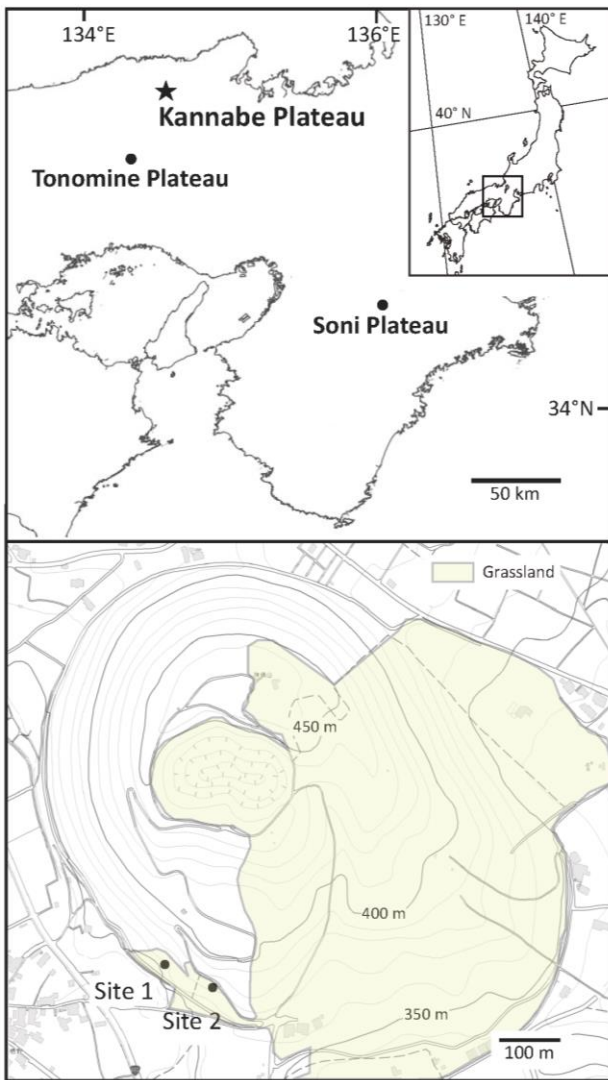


**Figure 1** Map of central Japan (top) showing the sites where phytolith and macrocharcoal in cumulative soils were examined in this study (Kannabe Plateau) and in previous studies (Soni Plateau and Tonomine Plateau). Topographic map of Kannabe Plateau (bottom) showing the locations of sampling points in this study.

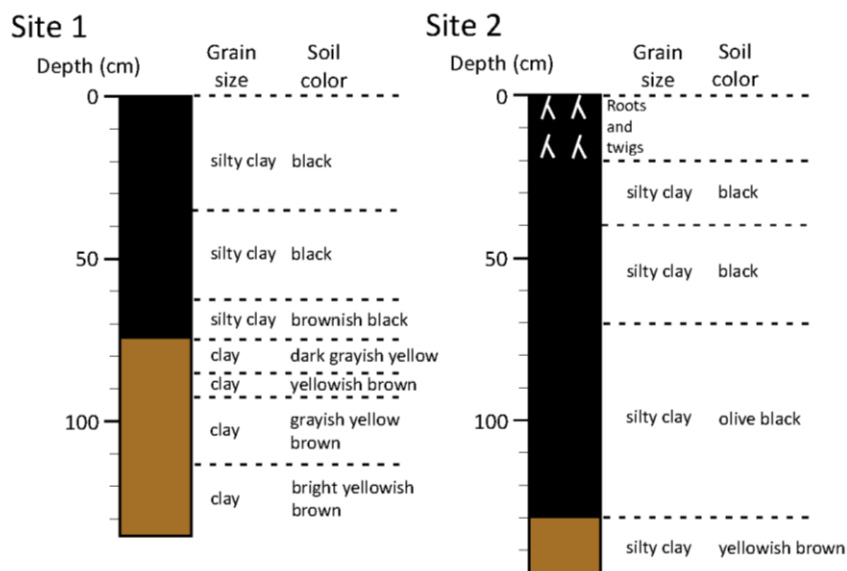
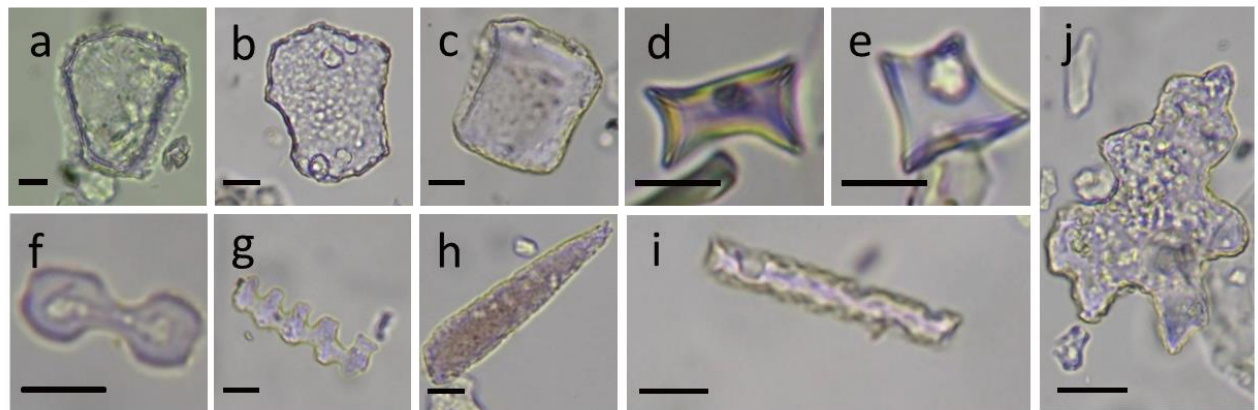


**Figure 2** Columnar sections of sites 1 and 2 indicating grain size, soil color, and root abundance in respective soil layers.

**Table 1** Radiometric soil ages on the Kannabe plateau. The  $^{14}\text{C}$  ages were calibrated to the calendar year using the program Calib Rev 7.1 (<http://calib.org/calib/>) and the IntCal13 calibration dataset.

Site number	Depth	$^{14}\text{C}$ age	Cal BP year ( $2\sigma$ )	$\delta^{13}\text{C}$ (‰)	Material	Code No.
1	15–35 cm	2200 ± 30 BP	2315 – 2135 cal. BP	–22.3	macrocharcoal	Beta-455524
1	69–75 cm	7640 ± 30 BP	8515 – 8385 cal. BP	–19.3	macrocharcoal	Beta-455525
1	125–135 cm	9210 ± 30 BP	10490 – 10260 cal. BP	–21.7	soil	Beta-455527
2	20–40 cm	1360 ± 30 BP	1335 – 1190 cal. BP	–21.2	macrocharcoal	Beta-455526
2	130–148 cm	8170 ± 40 BP	9255 – 9015 cal. BP	–19.8	soil	Beta-455528



Scale bar: 10  $\mu\text{m}$

**Figure 3** Microphotographs of main phytolith morphotypes collected from cumulative soils in this study. Scale bar is 10  $\mu\text{m}$ . a: *Pleioblastus*-type (bulliform cell) b: *Sasa*-type (bulliform cell) c: *Andropogoneae*-type (bulliform cell) d: *Bambusoideae* (short cell) e: Rondel f: Bilobate (short cell) g: Cylindrical polylobate h: Acicular i: Elongate j: Jigsaw puzzle-shaped.

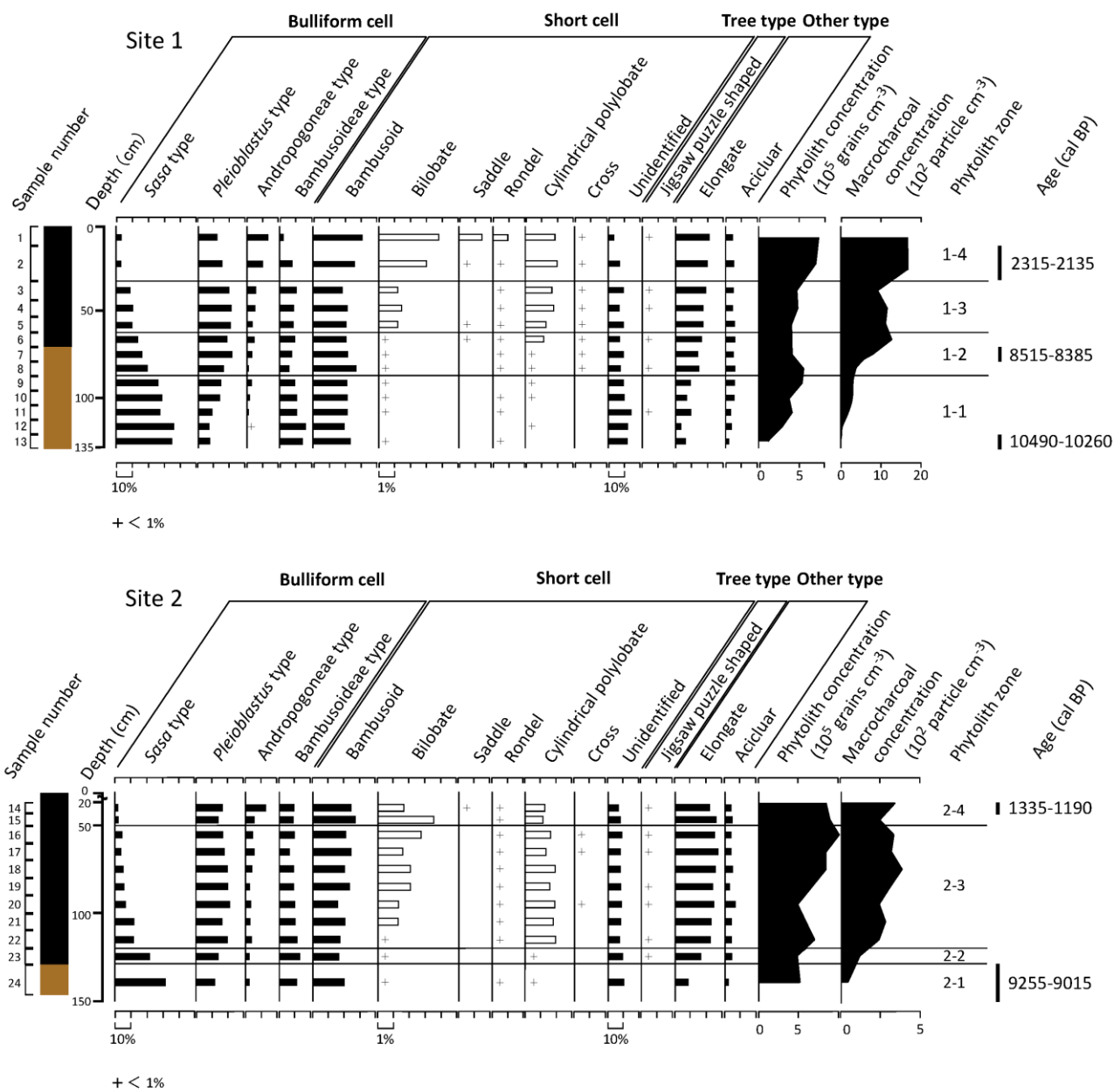


**Figure 4** Percent occurrence of respective phytolith morphotypes and concentrations of all phytolith morphotypes and macrocharcoal from sites 1 and 2 on the Kannabe Plateau.

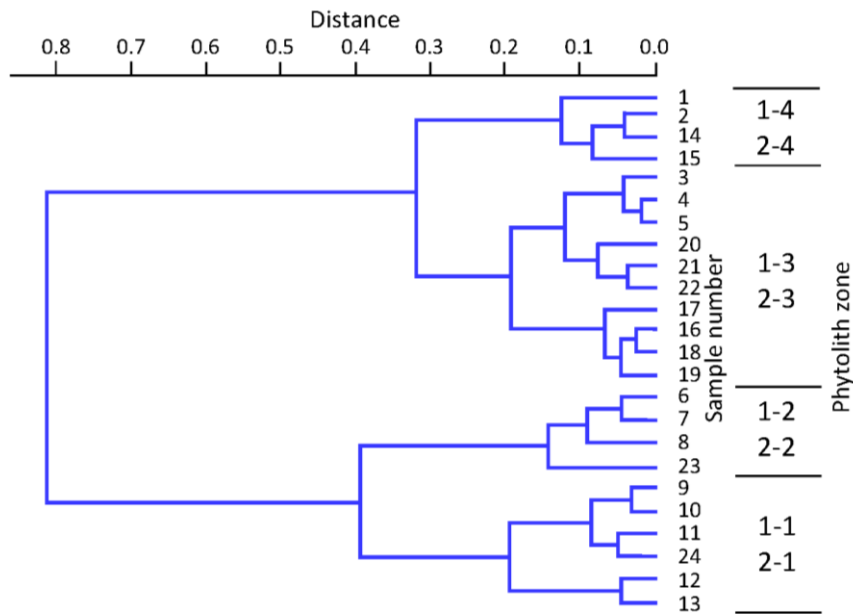


**Figure 5** Result of cluster analysis for phytolith assemblages (percentages of respective phytolith types, except for an unidentified phytolith) at sites 1 and 2.

**Table 2** Spearman's correlation coefficient between the percentage of each phytolith type and macrocharcoal concentration at respective sites in central Japan. KN is Kannabe Plateau (this study), SN is Soni Plateau (Okunaka et al., 2012), TN is Tonomine Plateau (Inoue et al., 2016).

	<i>Sasa</i>	<i>Pleioblastus</i>	<i>Andropogoneae</i>	<i>Bambusoid</i>	<i>Bilobate</i>	<i>Elongate</i>
KN site1	-0.93*	0.55*	0.92*	0.29	0.84*	0.91*
KN site2	-0.62*	0.51	0.53	0.23	0.58	0.42
SN site1	0.12	-0.55	0.95*	-0.69	0.79*	-0.81*
SN site2	0.52	-0.40	0.98*	-0.26	0.26	-0.60
TN site1	-0.31	0.52	0.69	-0.86*	0.36	-0.38
TN site2	-0.95*	-0.12	0.86*	0.48	0.26	-0.33

\*  $p < 0.05$